

PHOTOVOLTAIC SOLAR FARM WITH HIGH DYNAMIC PERFORMANCE ARTIFICIAL INTELLIGENCE BASED ON MAXIMUM POWER POINT TRACKING WORKING AS STATCOM

MOHAMMED OMAR BENAÏSSA, SAMIR HADJERI, SID AHMED ZIDI, YUCEF ISLAM DJILANI KOBIBI

Key words: Adaptive neuro fuzzy inference system (ANFIS), Static synchronous compensators (STATCOM), IEEE 14 bus test system, Maximum power point tracking (MPPT), Perturb and observe (P&O), Photovoltaic (PV) solar farm, Voltage regulation, Voltage source converter (VSC).

The present work is willing to enlarge the field of using the solar energy power generation in order to take better advantage of the sun radiation. In this paper a particular attention has been paid to the dynamic behavior of the grid connected PV system, against voltage sag and voltage swell caused respectively by adding a load and then removing the same load, the analysis has been done on IEEE 14 bus system. As an alternative to these irregular working conditions, the voltage source converter is a key component of the PV system with the purpose of providing voltage support by generating or absorbing reactive power at the point of common coupling, which makes it act as a real STATCOM. This novel usage of PV solar farm can keep the bus voltages at wanted level without requiring any extra voltage control devices that could increase the whole transmission system cost.

On the other hand the efficiency of photovoltaic generator can be improved by forcing the panel to operate at its maximum power point, this function is guaranteed by the maximum power point tracking (MPPT), in fact numerous techniques are described in the literature where the perturb and observe seems to be the simplest and commonly used method, however it has many disadvantages. In this paper adaptive neural fuzzy inference system (ANFIS) based MPPT method combines the ability of fuzzy logic to handle imprecise data and the learning abilities of artificial neural networks. It is found that this technique can precisely track the maximum power point under various irradiance and temperature conditions. Simulation results using Matlab/Simpower systems toolbox show an excellent waveforms quality and high performance dynamic behavior compared to the perturb and observe technique.

1. INTRODUCTION

Nowadays, the world pays growing attention to renewable energy sources, clean and practically inexhaustible [1], in particular solar energy hold a special place mainly because its financial benefits, in fact the price of PV panels has declined 99 % over the last four decades and has dropped by three fourths, helping global PV installations grow 50 % per year [2]. Some of the present day loads have a very complex and unpredictable nature. This includes a big component of industrial loads which are reactive in nature. Therefore, it is essential to support at least the reactive power demand through local generation [3], to avoid disastrous situations that would deteriorate the quality of electricity and cause considerable damage that may lead to the blackout in the worst cases. Well defined standards are already in place for governing voltage regulation and reactive power compensation such as IEEE 1860-2014, specify that actual service voltage must in no case exceed the standard limits of $\pm 5\%$ in order to maintain the voltage within tolerance under changing load conditions.

Reactive power is a major influencing parameter in ac systems due to its impact on the line voltage profile [3]. Beforehand IEEE 1547 didn't allow injecting the reactive power by the distribution generators into the electrical power system. But, due to the fast advancement in the technology the earlier version IEEE 1547 was revised as IEEE 1547.8, which is expected to permit the injection of reactive power into the grid system [4]. A. Di-Fazio *et al.* [5] have recommended the use of PV-grid inverters for reactive power compensation. R. K.Varma *et al.* [6] have reported that the PV-STATCOM improves the power

transmission limits which would have otherwise required expensive additional equipment such as, series/shunt capacitors, or separate flexible alternating current transmission system (FACTS) controllers, substantially in the night and also in the day. As a matter of fact one can conclude that the role of the PV solar farm is not confined to generate real power but also it has other functions when it is associated with VSC inverter.

Furthermore, it is very important to operate PV energy conversion systems near maximum power point (MPP) to obtain the approximately maximum power of PV generator [7], in fact there are several methods for obtaining the maximum power of the photovoltaic generator [8], the most commonly used methods are: perturb and observer (P & O) [9], incremental conductance (INC) [10, 11], fuzzy logic control (FLC) [12, 13], artificial neural network (ANN) [14]. Other studies have investigated the amalgamation of the (FLC) and (ANN), termed adaptive neuro fuzzy inference system (ANFIS) control such as in [15, 16], the latter has shown an impressive optimization and adaptation abilities.

This paper is an extension of a previous work originally reported in [17]. In addition to enhance the power injected into the utility grid by using the ANFIS-based MPPT, the present work proposes a very effective means to ensure the control of the voltage at PCC.

In light of the above research line the current work investigates mainly the dynamic performance of a PV solar farm associated to VSC operating as STATCOM under rapidly changing environmental conditions. The considered PV system is connected to IEEE-14 bus test system via point of common coupling (PCC). Simulation results obtained show that it is possible to develop a decoupled

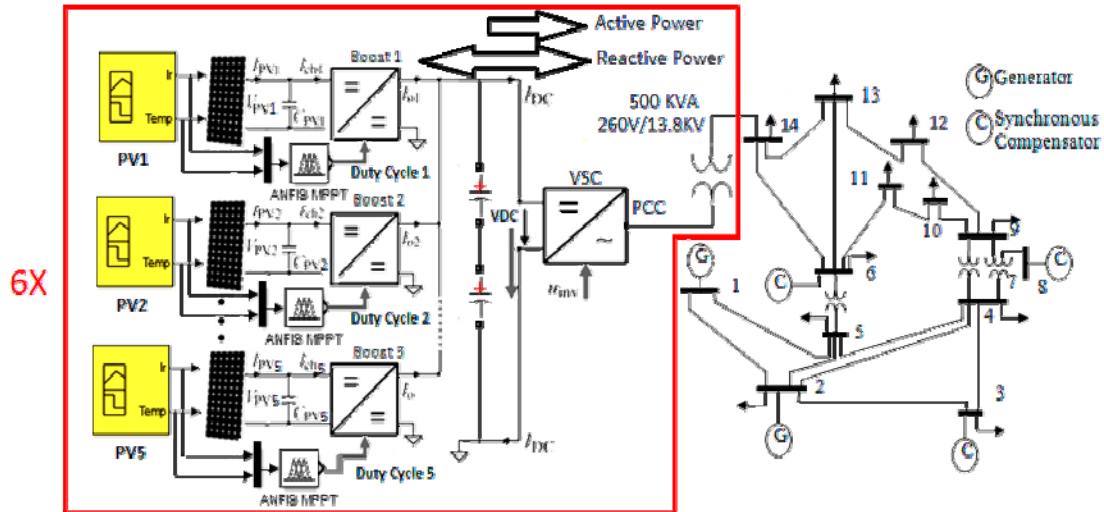


Fig. 1 – Schematic single line diagram of proposed PV-VSC integrated in IEEE-14 bus test system.

controller, which is able to compensate local loads reactive power and keep the grid voltage profile within the strict limits imposed by the standard, also output active power stably and effectively.

2. SYSTEM DESCRIPTION

Simulation studies has been done on the well recognized IEEE 14-bus system that contains 14 transmission lines, 5 generators, 11 static loads and 4 transformers. Base MVA is taken as 100 and base system voltage is 13.8 kV [18]. Significant attention has been paid in recent times to find out the best possible and the optimum location of the FACTS devices, M. Rani *et al.* [18] have stressed the need for connecting the STATCOM at bus 14 because it represents the weakest bus and introducing reactive power at bus 14 can improve voltage stability margin. Similarly in our case we opted for connecting the PV solar farm at bus 14 as shown in Fig. 1. The considered solar photovoltaic plants was designed to produce energy to be send to the grid via a dc-dc converter, however its peak value can't be reached without the presence of what we called commonly the MPPT [19]. In this paper solar irradiance and temperature are taken as input for the ANFIS based MPPT controller and the duty cycle of PWM as an output.

Furthermore, the voltage source converter (VSC) which is connected to the secondary side of a coupling transformer of 500 kVA and 260 V / 13.8 kV, can ensure two major functions, the first one is converting the dc voltage of 500 V delivered by the boost converter to an ac voltage of 260 V, the second one is maintaining voltage profile at PCC, to achieve this reactive power management is essential.

3. PV SYSTEM

The PV solar farm represented in this paper can generate a maximum power of $(6 \times 5 \times 100 \text{ kW} = 3 \text{ MW})$ at standard test conditions (STC). It consists of 6 plants of photovoltaic arrays. Each plant comprises 5 arrays of 100 kW work in parallel. Each array consists of 64 strings of 5 series-connected 315.072 W modules connected in parallel $(64 \times 5 \times 315.072 \text{ W} = 100.8 \text{ kW})$.

Manufacturer specifications for the module « SPR-315E-WHT-D » are listed in Table 1. The PV array block has two inputs that allow you varying sun irradiance (input 1 in W/m^2) and temperature (input 2 in $^{\circ}\text{C}$). The irradiance and the temperature profile are defined by a signal builder block which is connected to the PV array input [20]. The characteristics I - V and P - V of one module SunPowerSPR-315E-WHT-D type are represented in Fig. 2 [17].

Table 1

Specifications of SunPower SPR-315E-WHT-D PV module

Model name	SunPower SPR-315E-WHT-D
No. of cells per module	96
Open circuit voltage (V_{OC})	64.6 V
Short circuit current (I_{SC})	6.14 A
Maximum power voltage (V_{mp})	54.7 V
Maximum power current (I_{mp})	5.76 A
Maximum power point (MPP)	315.072 W

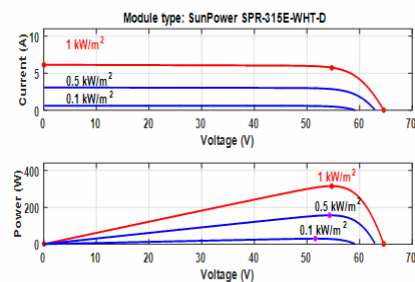


Fig. 2 – I - V and P - V characteristics of single module at 25 $^{\circ}\text{C}$ and varying irradiance.

The characteristics of PV array constituted of 5 series modules and 64 parallel strings are shown in Fig. 3.



Fig. 3 – Array type: Sun Power SPR-315E-WHT-D, 5 series modules, 64 parallel strings.

4. ANFIS-BASED MPPT CONTROL STRATEGY

In the present work the neural network has been combined with fuzzy logic, the main aim of concept of hybridization is to overcome the weakness in one technique called ANFIS, while applying it and bringing out the strength of each of them [21, 22]. ANFIS uses neural network to develop the fuzzy membership functions and rule base through the training process [23]. Here the MPPT detects the inputs G and T , and selects the duty cycle corresponding to them and send it to the PWM controller; five layers have been utilized where in each layer every node executes the same function as shown in Fig. 4. Each input has five membership functions so that there are twenty five fuzzy rules derived. The initial membership functions are chosen as trapezoidal type (see Fig. 5). To perform the training process in ANFIS, the data is collected using the P&O method for various climatic conditions. Figure 6 shows the generated surface with the three dimensional plot for the learned ANFIS network.

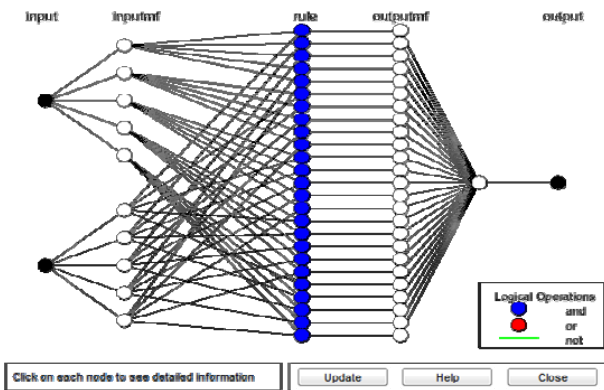


Fig. 4 – ANFIS-based MPPT controller structure.

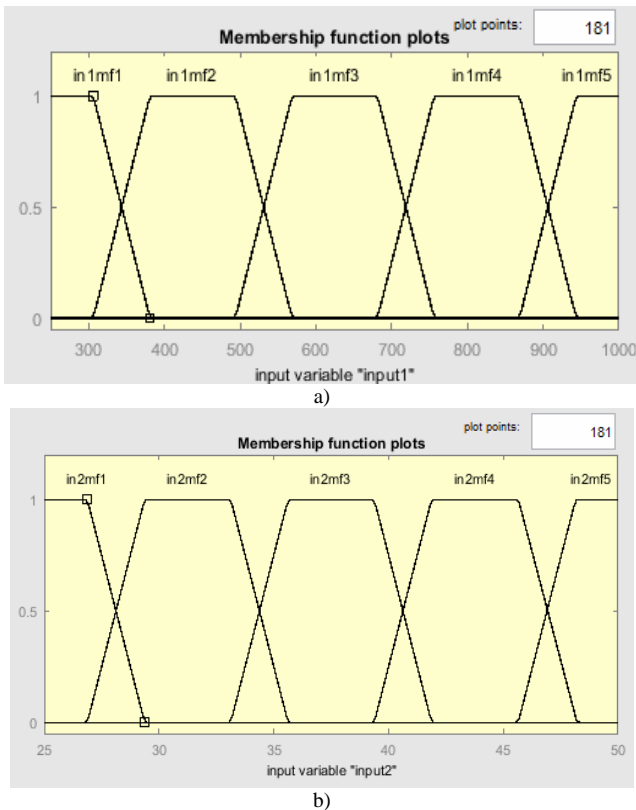


Fig. 5 – Input membership functions of ANFIS: a) Irradiance; b) Temperature.

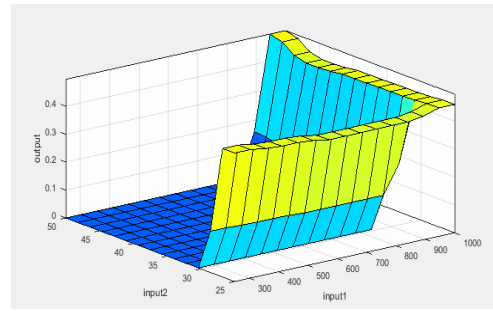


Fig. 6 – Surface between two inputs and one output.

5. VOLTAGE SOURCE CONVERTER CONTROL STRATEGY

The STATCOM considered in this chapter is a voltage source converter that from a given input of dc voltage produces a set of 3-phase ac-output voltages. The control technique of the VSC based on the concept of vector control can control the reactive power and the active power independently (decoupling). It is composed of two proportional-integral (PI) based voltage-regulation loops, one loop regulates the PCC voltage, while the other maintains the dc bus voltage across the voltage source converter at a constant voltage level [24].

The active and reactive powers can be determined as follows:

$$P = \frac{3}{2} V_d I_d \tag{1}$$

$$Q = \frac{3}{2} V_q I_q \tag{2}$$

where I_d and I_q are the d and q currents corresponding to I_a, I_b, I_c , and V_d, V_q represent d and q axis voltage corresponding to V_a, V_b, V_c .

The phase-locked loop (PLL) is used to provide the basic synchronizing signal which is the reference angle to the measurement system. Measured bus line voltage V_{ac} is compared with the reference voltage V_{ref} , and the voltage regulator provides the required reactive reference current I_{qref} (see Fig. 7). Also the reactive current I_q of STATCOM and reference current I_{qref} , are compared and the current regulator provides the angle phase shift of the inverter voltage with regard to the system voltage as its output [25].

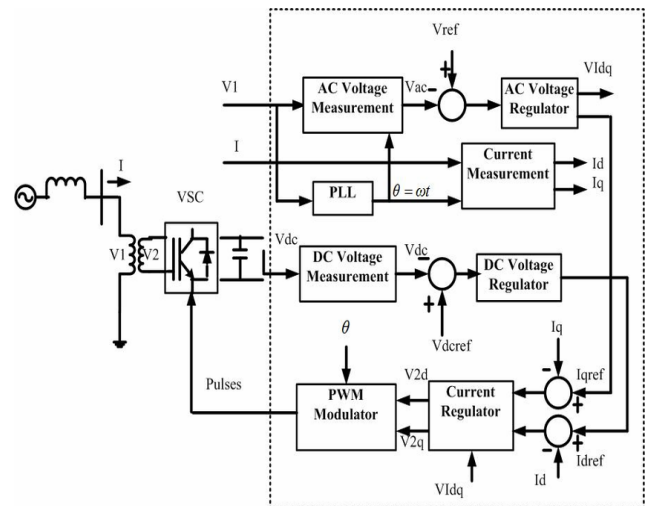


Fig. 7 – Block of control strategy for VSC

The dc measurement system in Fig. 7 provides the measurement of the dc voltage V_{dc} . The ac voltage measurement and current measurement systems in the same figure measure the d and q components of ac positive-sequence voltage and currents to be controlled, respectively.

A STATCOM with VSC using PWM inverters has been used in this study. Figure 7 shows a single-line diagram of a VSC and its control system block diagram [26].

6. SIMULATION RESULTS AND DISCUSSION

The considered grid connected PV system is assumed working under fast and slow modifications of both the environmental conditions irradiance, and the ambient temperature as shown respectively in Fig. 8.

At $t = 0$ s, the voltage of the network is equal to 1 pu (see Fig. 9) which is identical to the reference value, consequently, the voltage source converter is initially floating (STATCOM is inactive), it does not absorb nor provide reactive power to the network, thus $I_q = 0$ (see Fig. 11) and the total reactive power injected into the grid is zero (see Fig. 12). From $t = 0.5$ s to $t = 1.5$ s, the voltage is decreased by 7.2 % > 5 % (lower limit specified by the standard), hence the voltage is equal to 0.928 pu (see Fig. 9), due to connecting an inductive load which is unacceptable, the VSC must generate reactive power to enhance the voltage value (I_q changes from 0 to -1 pu) see Fig. 11 and (Q changes from 0 to 2.6 Mvar) (see Fig. 12), consequently the voltage is increased to 0.971 pu which is acceptable (see Fig. 10). After 1.5 s, the inductive load has been removed so that the voltage returns to its nominal value 1 pu. At $t = 2$ s to 3 s, the voltage is increased by 7.2 % > 5 % (upper limit specified by the standard), hence the voltage is equal to 1.072 pu (see Fig. 9) due to disconnecting an inductive load which is unacceptable, the VSC reacts this time by absorbing reactive power ($Q = -2.7$ Mvar, see Fig. 12), consequently the voltage is decreased to 1.029 pu which is acceptable (see Fig. 10). Note that when the VSC change from capacitive to inductive operation, the modulation index of the PWM inverter is decreased from 0.93 to 0.77 (see Fig. 13).

The total real power of PV farm which will be transferred to the grid without MPPT controller, with P&O MPPT, and ANFIS MPPT for the selected temperature and irradiance levels is given in Fig. 14, it is clearly observed that the gain in the real power is significantly high in case of ANFIS MPPT compared to conventional P&O MPPT, in fact the maximum power drawn at ambient temperature 25°C and standard irradiance 1000 W/m² is 2980 kW with ANFIS MPPT, whereas in case of P&O MPPT it can hardly reach 2900 kW. Also we can say that the ANFIS MPPT has better dynamic performance compared to P&O MPPT as shown at 2.5 s where the overshooting of the last one is greater. Moreover, the duty cycle graph of Fig. 15 has shown that more oscillations have occurred in case of P&O MPPT compared to ANFIS MPPT; hence ANFIS is the best in tracking MPP than conventional P&O. As a result the change of the duty cycle value is very small as well as the environmental parameters change, because it has a small oscillations then the output dc voltage change of the converter is also small (see Fig. 16), while Fig. 17 represents the active current which is simply the image of

the real power (see Fig. 14).

Note. Sign convention:

- I_d positive: the converter generates active power (inverter mode) = active power P positive.
- I_q positive: the converter absorbs reactive power (inductive mode) = reactive power Q negative.

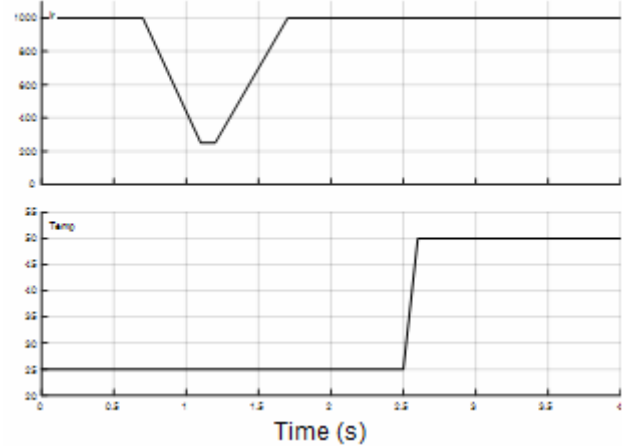


Fig. 8 – The change of solar irradiation and temperature in simulation.

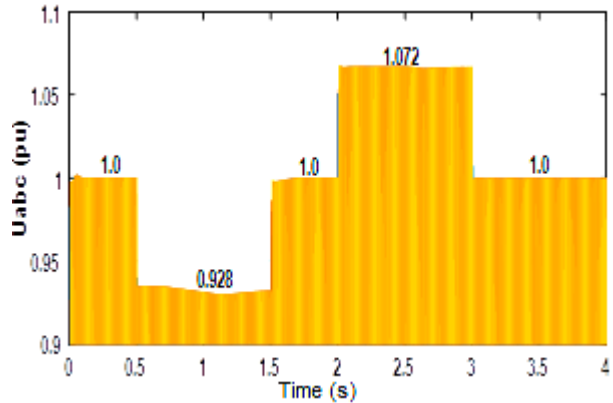


Fig. 9 – Output 3-phase a voltage at PCC without PV system compensation.

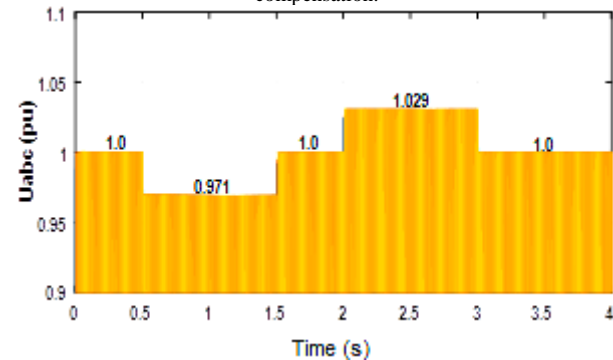


Fig. 10 – Output 3-phase AC voltage at PCC with PV system compensation.

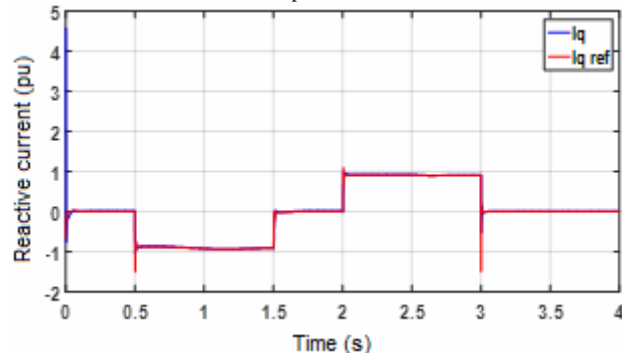


Fig. 11 – Reactive current.

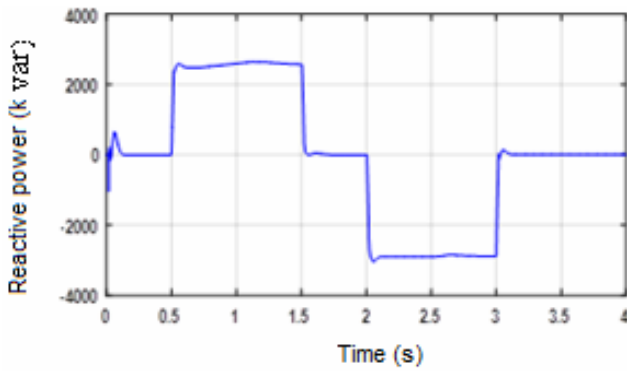


Fig. 12 – Injected total reactive power.

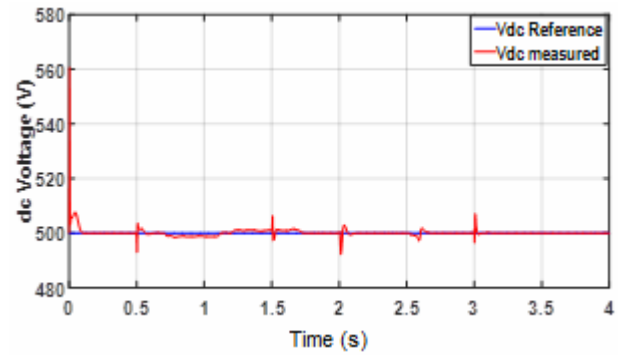


Fig. 16 – Dc output voltage of boost converter.

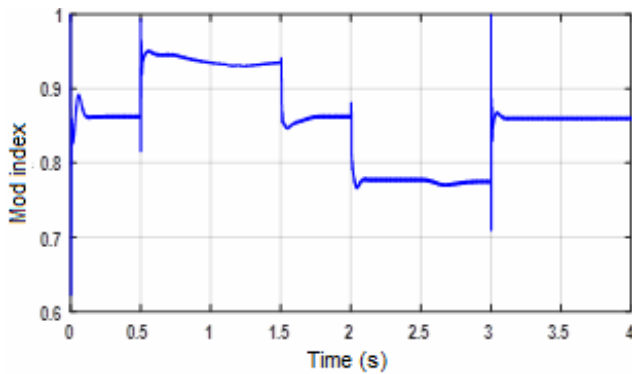


Fig. 13 – Modulation index of VSC.

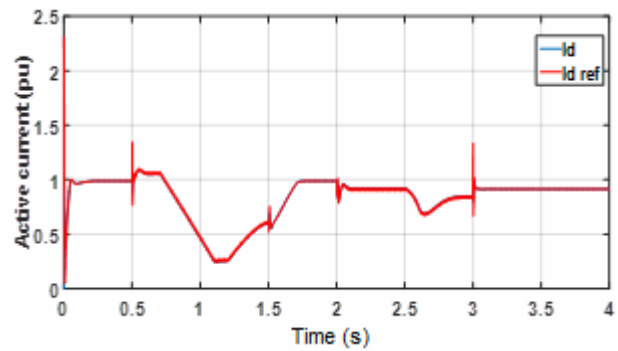


Fig. 17 – Active current.

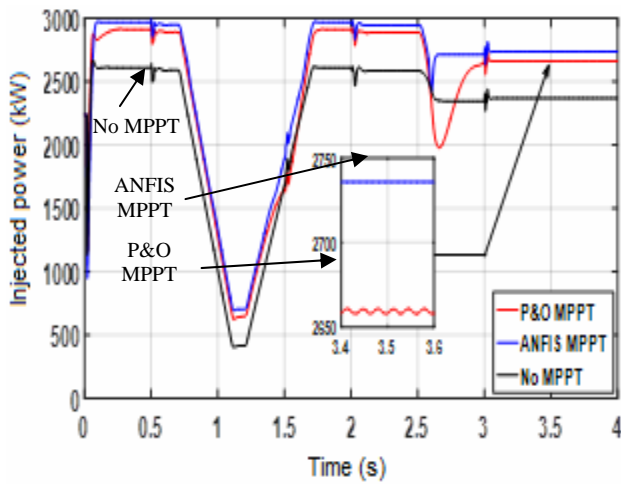


Fig. 14 – Injected total real power.

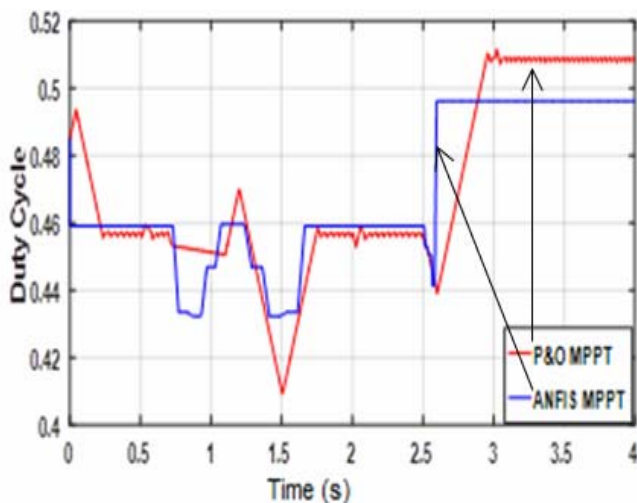


Fig. 15 – Duty cycle of the boost converter.

7. CONCLUSIONS

From the analysis presented above, the following conclusions can be derived:

- Grid connected PV system can perform two functions the first one is to supply the energy to the grid as long as the sun radiation reaches the photovoltaic cells, in addition it can operate as a STATCOM and regulate the voltage to a desired level whenever necessary.
- The PV solar farm can give a remarkable results meeting the reactive power demand under different loading conditions through the VSC.
- The ANFIS-based MPPT control scheme is very efficient to track the maximum available power from the PV module with regards to perturb and observe technique; also it has much smaller changes in the real power value injected into the grid under varying weather conditions.

Received on May 28, 2017

REFERENCES

1. antoneta i. bratcu, i. munteanu, s. bacha, d. picault, b. raison, *cascaded DC-DC converter photovoltaic systems: power optimization issues*, IEEE Trans. Industrial Electronics, **58**, 2, pp. 403–411 (2011).
2. W. R. Sultana, S. K. Sahoo, S. Sukchai, S. Yamuna, D. Venkatesh, *A review on state of art development of model predictive control for renewable energy applications*, Renewable and Sustainable Energy Reviews, **76**, pp. 391–406 (2017).
3. R. G. Wandhare, V. Agarwal, *Reactive power capacity enhancement of a PV- grid system to increase PV penetration level in smart grid scenario*, IEEE Trans. Smart Grid, **5**, 4, pp. 1845–1854 (2014).

4. L. Naik, K. Palanisamy, *A dual operation of PV-Statcom as active power filter and active power injector in grid tie wind-PV system*, International journal of renewable energy research, **5**, 4, pp. 978–982 (2015).
5. A. Di-Fazio, G. Fusco, M. Russo, *Decentralized control of distributed generation for voltage profile optimization in smart feeders*, IEEE Trans. Smart Grid, **4**, 3, pp. 1586–1596 (2013).
6. R. K. Varma, S. A. Rahman, T. Vanderheide, *New control of PV solar farm as STATCOM (PV-STATCOM) for increasing Grid power transmission limits during night and day*, IEEE Trans. Power Delivery, **30**, 2, pp. 755–763 (2015).
7. W. NianCHun, S. Zuo, K. Yukita, Y. Goto, K. Ichiyanagi, *Research of PV model and MPPT methods in Matlab*, IEEE Power and Energy Engineering Conference (APPEEC), Asia-Pacific, 2010.
8. M. N. Amrani, A. Dib, S. Alem, *Optimization des performances d'un système de pompage photovoltaïque par Neuro Floue et le Contrôle Direct du Couple*, Rev. Roum. Sci. Techn – Électrotechn. et Énerg., **59**, 3, pp. 279–289 (2014).
9. N. Fernia, G. Petrone, G. Spagnuolo, M. Vitelli, *Optimization of perturb and observe maximum power point tracking method*, IEEE Trans. Power. Electron., **20**, pp. 963–973 (2005).
10. D. C. Huynh, M. W. Dunnigan, *Development and comparison of an improved incremental conductance algorithm for tracking the MPP of a solar PV*, IEEE Trans. Sustainable Energy., **7**, 4, pp. 1421–1429 (2016).
11. P. S. Skider, N. Pal, *Incremental conductance based maximum power point tracking controller using different Buck-Boost converter for solar photovoltaic system*, Rev. Roum. Sci. Techn – Électrotechn. et Énerg., **62**, 3, pp. 269–275 (2017).
12. A. Attou, A. Massoum, M. Chadli, *Comparison study of two tracking methods for photovoltaic systems*, Rev. Roum. Sci. Techn – Électrotechn. et Énerg., **60**, 2, pp. 205–214 (2015).
13. A. El Khateb, N. Abd Rahim, J. Selvaraj, M. N. Uddin, *Fuzzy-logic-controller-based SEPIC converter for maximum power point tracking*, IEEE Trans. Industry Applications., **50**, 4, pp. 2349–2358 (2014).
14. Lina M. Elobaid, A. K. Abdelsalam, E. E. Zakzouk, *Artificial neural network-based photovoltaic maximum power point tracking techniques: a survey*, IET Renewable Power Generation, **9**, 8, pp. 1043–1063 (2015).
15. A. Semmah, H. Hamdaoui, A. Ayad, Y. Ramdani, *Commande floue et Neuro-Floue d'un dispositif facts*, Rev. Roum. Sci. Techn – Électrotechn. et Énerg., **54**, 2, pp. 195–204 (2009).
16. H. Abu-Rub, A. Iqbal, S. Moin Ahmed, F. Z. Peng, Y. Li, G. Baoming, *Quasi-Z-source inverter-based photovoltaic generation system with maximum power tracking control using ANFIS*, IEEE Trans. Sustainable Energy, **4**, 1, pp. 11–20 (2013).
17. M.O. Benaissa, S. Hadjeri, S.A. Zidi, Y.I. Djilani Kobibi, *A Comparative investigation of maximum power point tracking techniques for grid connected PV system under various weather conditions*, 5th International Conference on Electrical Engineering - Boumerdes (ICEE-B), Algeria, 2017.
18. M. Rani, A. Gupta, *Steady state voltage stability enhancement of power system using facts devices*, IEEE Power India International Conference (PIICON), Delhi, India, 2014.
19. R. B. A. Koad, A. F. Zobaa, A. El-Shahat, *A novel MPPT algorithm based on particle swarm optimization for photovoltaic systems*, IEEE Trans. Sustainable Energy, **8**, 2, pp. 468–476 (2017).
20. M.O. Benaissa, S. Hadjeri, S.A. Zidi, *Modeling and Simulation of grid connected PV generation system using Matlab/Simulink*, International journal of power electronics and drive systems, **8**, 1, pp. 392–401 (2017).
21. A. Chikh, A. Chandra, *An optimal maximum power point tracking algorithm for PV systems with climatic parameters estimation*, IEEE Trans. Sustainable Energy, **6**, 2, pp. 644–652 (2015).
22. H. Abu-Rub, A. Iqbal, M. Ahmed, *Adaptive neuro-fuzzy inference system-based maximum power point tracking of solar PV modules for fast varying solar radiations*, Int. J. of Sustainable Energy, **31**, 6, pp. 383–398 (2012).
23. Y. T. Chu, L. Q. Yuan, H. H. Chiang, *ANFIS-based maximum power point tracking control of PV modules with DC-DC converters*, IEEE International Conference on Electrical Machines and Systems (ICEMS), Pattaya city, Thailand, 2015.
24. R. K. Varma, V. Khadkikar, R. Seethapathy, *Nighttime application of PV solar farm as STATCOM to regulate grid voltage*, IEEE Trans. Energy Conversion, **24**, 4, pp. 983–985 (2009).
25. Y. Xu, F. Li, *Adaptive PI Control of STATCOM for Voltage Regulation*, IEEE Trans. Power Delivery, **29**, 3, pp. 1002–1011 (2014).
26. J. Shi, A. Kalam, A. Noshadi, P. Shi, *Genetic Algorithm Optimised Fuzzy Control of D-STATCOM for Improving Power Quality*, IEEE Australasian Universities Power Engineering Conference (AUPEC), Perth, WA, Australia, 2014.